Aerosol and Air Quality Research, 9: 344-351, 2009

ISSN: 1680-8584 print / 2071-1409 online
doi: 10.4209/aaqr.2009.01.0008

Retrieval of Columnar Aerosol Size Distributions from Spectral Attenuation Measurements over Central Himalayas

U.C. Dumka[1,2*], Ram Sagar[1], P. Pant[1]

[1] *Aryabhatta Research Institute of Observational Sciences, Manora Peak, Nainital, India*
[2] *Tata Institute of Fundamental Research (TIFR), National Balloon Facility, Hyderabad, India*

ABSTRACT

Extensive measurements of spectral aerosol optical depths (AODs) were made at Manora Peak, Nainital (29.4°N, 79.5°E, ~1958 m above mean sea level) in the central Himalayas, using a ten channel multi-wavelength solar radiometer during January 2002 to December 2005. Using these spectral AOD values, the columnar size distribution [CSD; $n_c(r)$] function of aerosols have been derived. The CSD, retrieved from spectral AODs are, in general, bimodal (combination of power law and unimodal log normal distribution) with a prominent secondary (or coarse) mode occurring at a fairly large value of radius ($r > 0.5$ μm), while the primary (or fine) mode either does not appear explicitly or perhaps occurs below the radius ≅ 0.1 μm. The bimodal nature of CSDs indicates the presence of fine as well as coarse mode aerosols over the observational site. The effective radius, total aerosol number content and columnar mass loading computed from deduced CSD shows minimum values during winter (November to February) and maximum during summer (March to June) months. The share of sub micron and super micron aerosols to the total aerosol number concentration (N_t) indicates the dominance of sub micron aerosols to the N_t and it accounts for > 90% during the study period.

Keywords: Extinction coefficients; Optical depth; Size distribution.

INTRODUCTION

Size distribution is one of the most prominent properties of atmospheric aerosols from the stand point of climate impact. Most of the effects of aerosols can be understood only with the knowledge of its size distribution. Many processes in the Earth's atmosphere concerning these aerosols are closely related to the aerosol size distribution therefore it is quite essential to understand the size distribution of aerosols as far as their effect on both climate (Charlson *et al.,* 1987; Russell *et al.,* 1994) and human health (Künzli *et al.,* 2000) are concerned. The effect of aerosols on climate is generally classified into direct and indirect effect. The direct effect comes from the capability of aerosols to scatter and absorb the incoming short wave and out going long wave solar radiation (Charlson *et al.,* 1992), while the indirect effect is a result of the ability of aerosols to act as cloud condensation nuclei; thereby affecting the cloud droplet size distribution, droplet concentration, optical properties, precipitation rate and lifetime of clouds (Twomey, 1977; Ackerman *et al.,* 2000; Rosenfield, 2000). Furthermore, the aerosol size distributions along with particle refractive index and shape are one of the most important parameters, which determine their optical properties such as optical thickness, asymmetry factor, scattering phase function, single scattering albedo and other useful information needed in the aerosol radiative forcing estimation.

In India a number of studies were carried out on the aerosol size distributions using in-situ measurements. However, most of these studies are focused to the low altitude (< 1 km amsl) locations that encompass either urban/semi-urban landmass or oceans adjacent to densely populated and polluted coastal belt (Moorthy *et al.,* 1997; Nair and Moorthy, 1998; Moorthy and Satheesh, 2000; Srivastava *et al.*, 2008) and also the area nearby Indo-Gangetic Plains (Day *et al.,* 2004; Singh *et al.,* 2004). The site specific nature of aerosol properties is clearly reported by Ganesh *et al.* (2008). Such studies are lacking over the northern part of the Indo-Gangetic Plains, particularly in the Himalayan regions. Investigation from the remote, sparsely inhabited regions have the importance of providing a sort of background against which the urban impacts can be compared (Pant *et al.,* 2006). From this perspective, observations from high altitude stations have prime importance. There is no such study at a high altitude (~2 km amsl) in the northern part of Indian subcontinent except recently started station at Nainital, located in the Central Himalayas (Sagar *et al.,* 2004). In the present investigation we present the columnar size distribution (CSD) function inferred by numerical inversion of spectral aerosol optical depth (AOD) measurements over a period of four years (January 2002 to December 2005). The results and implications of these studies are discussed in the manuscript.

PHYSICAL FEATURE AND GENERAL METEOROLOGICAL CONDITIONS

The observational site Manora Peak, Nainital (29.4° N, 79.5° E, ~1958 m amsl) is located in the Central Himalayas at an areal distance of ~20 km from the plains of northern India. It is ~3 km due southwest of the Nainital main city. The observational site is surrounded by the undulated topography from three sides, east, north and west while to the south it has a deep valley region (below the mountain peaks) of the northern Indian plains. Being the hilly terrain the site is free from any major industrial activities and urban impacts. It has thick vegetation of the Central Himalayas, with floating populations of around ~1 million. The

* Corresponding author. Tel.: +91-5942 233734 ext. 304;
Fax: +91-5942-233439.
E-mail Address: ucdumka@gmail.com; dumka@aries.ernet.in

observational site has a varied topography as shown in Fig. 1, where the color code represents topographical features of the region surrounding Nainital. The details on the geographical location and meteorological conditions over the site have also been reported in earlier papers (Sagar *et al.,* 2004; Dumka *et al.,* 2008).

EXPERIMENTAL DETAILS

Measurements of spectral aerosol optical depths (AODs) which characterize the integrated extinction of solar radiation suffered during its transit through the earth atmosphere were made by using a multi wavelength solar radiometer [MWR] (Gogoi *et al.,* 2009). The MWR makes continuous measurements of direct solar flux at 10 wavelength bands centered at 380, 400, 450, 500, 600, 650, 750, 850, 935 and 1025 nm, with FWHM 5 nm. The details of the instrument, method of data analysis and error budget are discussed in earlier papers (Sagar *et al.,* 2004; *Gogoi et al.,* 2009; Rana *et al.,* 2009). Estimates of columnar AODs were made regularly on all clear sky day conditions during four-year period (2002 to 2005) at Nainital. These are averaged to get the monthly mean AOD spectra. A total 38 AOD spectra, thus generated during the above period, formed the basic data set in the present study.

The experimental data considered of spectral AOD, carry information about the aerosol size distribution. Using these spectral AOD ($\tau_{p\lambda}$) values, the CSD function [$n_c(r)$] of aerosols have been determined by numerical inversion of the Mie integral equation,

$$\tau_{p\lambda} = \int_{r_1}^{r_2} \pi r^2 Q_{ext}(m,r,\lambda) n_c(r) dr \qquad (1)$$

where Q_{ext} is the aerosol Mie extinction efficiency parameter, which is a function of the aerosol complex refractive index (m), radius (r) and wavelength of the incident radiation (λ); $n_c(r)$ is the columnar number density of aerosols (in a vertical column of unit cross section in an infinitesimal radius range dr centered at r). In defining the $n_c(r)$ this way, it is implicitly assumed that the number size distribution is height invariant or averaged over the vertical column. The radii limits r_1 and r_2 to the integral are respectively the lower and upper cutoff radii of the particles, such that only those particles having sizes within the range r_1 to r_2 contribute significantly to Q_{ext}. Since the MWR measures only the directly transmitted flux, we used the spectral AODs and Eq. (1) to retrieve the columnar size distribution. The spectral AODs from the measurements and the corresponding errors formed the inputs. Eq. (1) is solved for $n_c(r)$, following the iterative inversion procedure described by King *et al.* (1978); King (1982), as applied by Moorthy *et al.* (1997). This technique provides fairly accurate information about the aerosol size distributions if the Lagrange multiplier, refractive index, and radius range are carefully selected (King, 1982), particularly when the $\tau_{p\lambda}$ spectra do not show large oscillations. The detailed application of this technique to the MWR data have been discussed by Moorthy *et al.* (1991); Saha and Moorthy (2004) and Gogoi *et al.* (2009). In the present study, we set r_1 = 0.05 μm and r_2 = 3.0 μm as optimal after performing a sensitivity analysis of the size range on Q_{ext} over the entire wavelength range of measurements used in the MWR to estimate $\tau_{p\lambda}$ (King, 1982; Moorthy *et al.,* 1997). The wavelength dependent complex refractive index of aerosols depends on the aerosol chemical composition and as such it is different for different types of aerosols. As the chemical composition was not available to us due to lack of facility, the values of refractive index as a function of wavelengths are taken from the literature for different types of aerosols (Shettle and Fenn, 1979), for estimating the Q_{ext} values in Eq. (1). The spectral AODs are re-estimated using the direct Mie equation, after each iteration, and are compared with the input AOD spectrum, and the solution are accepted only when the re-estimated AOD values agree with those from measurements within the measurement errors. As the measurement errors are used as input, the solutions are weighted by these errors with better accuracy around the size ranges sensitive to more accurate AOD measurements (King, 1982). The details of the retrieved CSDs, from the spectral AOD by means of inversion technique are presented in the following sections.

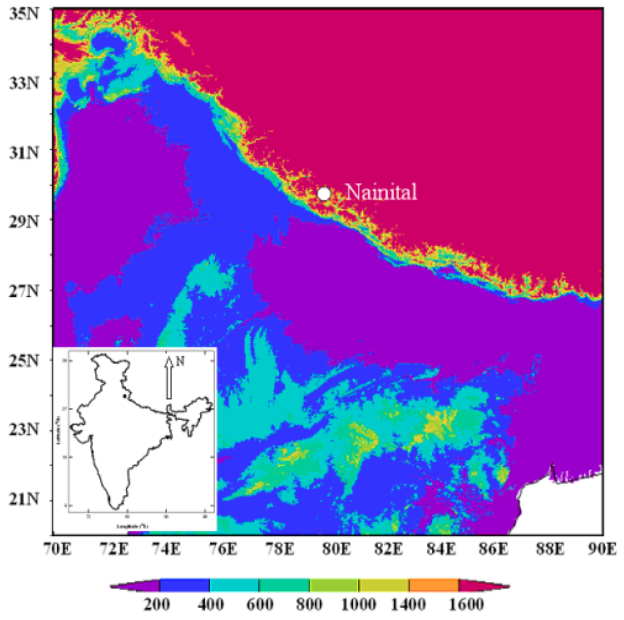

Fig. 1. The geographical location of Manora Peak, Nainital over the Indian subcontinent. The color code represents the topographical features (m) of the observational site.

RETRIEVED SIZE DISTRIBUTIONS AND ITS PARAMETERIZATION

By following the procedure discussed in preceding sections, $n_c(r)$ is retrieved from a set of spectral AOD measurements. The CSDs deduced by the inversion of spectral AOD are presented in a graphical form by plotting $n_c(r)$ against r on a log-log scale. The CSDs retrieved during the study period are examined for the general features. An examination of all the retrieved CSDs, revealed a bimodal [a combination of power law (PL) and unimodal (UM)] in nature. A typical example of such type of distribution is shown in Fig. 2. This type of size distribution is characterized by a secondary mode occurring at a fairly large value of radius (r > 0.5 μm), while the primary mode may not be well developed or occurs at or below the radius 0.1 μm because the lower radii limit used in the inversion processes is much higher than that. The peak number density for secondary mode is generally two to three orders less than the primary mode number density.

In order to understand the observed changes in the deduced CSDs in terms of physical parameters of the aerosols, as well as to present them in the form that can be used for computation, it is essential to parameterize the CDSs using proper analytical functions, which depend on the physical properties of aerosols such as geometric mean/mode radii (r_{mi}) and the geometric mean standard deviations (σ_{mi}). For this purpose we have used bimodal (PL + UM) log normal distribution using the equation:

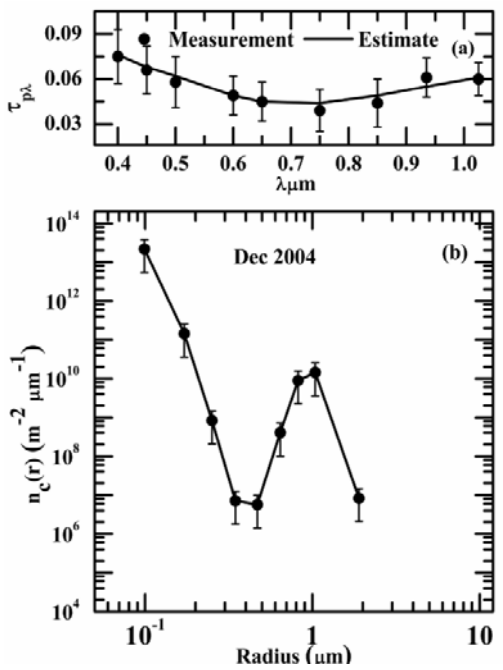

Fig. 2. (a) The input $\tau_{p\lambda}$ values estimated from the MWR measurements as the point with error. The continuous line represents $\tau_{p\lambda}$ values re-estimated using the retrieved CSDs. (b) typical example of CSD retrieved from monthly mean spectral AOD for the month of December 2004 at Nainital.

$$n_c(r) = N_{01} r^{-\upsilon} + \frac{N_{02}}{(2\pi)^{0.5}\sigma_2 r} exp\left[-\frac{1}{2}\left\{\frac{ln\, r - ln\, r_{m2}}{\sigma_2}\right\}^2\right] \quad (2)$$

where N_{01} and N_{02} are scaling parameters which depend on the aerosol concentration, r_{m2} and σ_2 are respectively the mode radii and standard deviation of the secondary mode and ν is power law index. By evolving a fit between the retrieved CSDs and appropriate analytical functions with minimum rms error, the power law index, mode radii and standard deviations are deduced as applicable. In addition to the above, the other parameters representing the physical state of the aerosols were estimated following the expressions:

$$\text{Effective Radius, } R_{eff} = \frac{\int_{r_1}^{r_2} r^3 n_c(r)dr}{\int_{r_1}^{r_2} r^2 n_c(r)dr} \quad (3)$$

For a given aerosol size distribution, R_{eff} is a measure of the total volume to area of aerosols and gives the radius of an equivalent mono-dispersion that would exhibit the same scattering properties (Moorthy *et al.,* 1997; Satheesh *et al.,* 1999; and reference cited therein)

$$\text{Columnar mass Loading, } m_L = \frac{4}{3}\pi\rho \int_{r_1}^{r_2} n_c(r) r^3 dr \quad (4)$$

where ρ is the density of aerosols, taken as 2.0 g/cm^3 (Junge, 1963).

$$\text{Columnar number density, } N_t = \int_{r_1}^{r_2} n_c(r)dr \quad (5)$$

The columnar content of the accumulation (N_a) and coarse mode (N_c) aerosols were also estimated, considering particles smaller than 0.5 μm in radius to represent the accumulation regime.

RESULTS

While dealing with the monthly, seasonal and spectral variation of AODs at Nainital, it has been observed that there is a systematic change in the wavelength dependence of τ_p from winter (November-February) to summer (March-June) months (Dumka *et al.,* 2008). These changes in spectral variation are indicative of the changes in CSD of aerosols. In the following paragraph, the above aspect are examined using CSDs retrieved from the λ dependence of τ_p values over Nainital and the results and implications are discussed.

Monthly and Seasonal Variation of CSDs

Representative CSDs for each month of the study period have been obtained by inverting the monthly mean $\tau_{p\lambda}$ values. The retrieved CSD generally show a steep fall in columnar number density $n_c(r)$ with increase in r from 0.05 μm (at the lower particle size; depicting an inverse power law type dependence), followed by a well defined secondary mode (coarse particle; depicting a unimodal type distribution) as shown in Fig. 2. At still larger size the number density $n_c(r)$ decreases again with r (see Fig. 2). The typical CSD obtained for December 2004 (Fig. 2) has two panels, the lower panel (b) representing the retrieved CSDs in a log-log scale, while the upper panel (a) depicts the measured AODs (solid points with error bars) along with the re-estimated AODs (continuous line) from the retrieved CSDs as shown in panel (b). In Fig. 2, the $n_c(r)$ decreases initially upto r = 0.5 μm, where it falls by six orders in magnitude from its value 10^{13}/m^2/μm at r = 0.07 μm. From r = 0.5 μm onwards the value of $n_c(r)$ increases gradually, reaching a secondary peak ($n_c(r) \sim 10^{10}$/m^2/μm) at r = 1.0 μm and then continuously decrease with r. In such type of CSDs, for the smaller size (accumulation/fine mode aerosols) particles, sometimes no mode is explicitly seen and at times its presence at radii below r_1 is indicated by the slanting nature of the CSD towards the smaller values of r. Thus, the slanting nature of the size distribution indicates the occurrence of a primary/fine mode at a value of r lower than the lower limit (r_1) as considered in the inversion process. This is also physically justifiable as the number density cannot increase indefinitely because of the processes like as coagulation, which limits the concentration of the sub micron aerosols. This leads to the formation of an accumulation mode aerosols (Hoppel *et al.,* 1990), by rapid transformation of smaller size aerosols to the larger ones.

In all, 38 such size distributions are obtained during the period of January 2002 to December 2005. It has been observed that all these retrieved CSDs can be analytically represented by a combination of power law and unimodal log normal distribution in nature in the optically active size range. The composite plots of monthly mean CSDs retrieved for each year are shown in Fig. 3, following the same convention as Fig. 2. The nature of all CSDs remains more or less same throughout the period under study.

As the aerosol properties over the Manora Peak, Nainital, have shown the well defined seasonal variations (Dumka *et al.,* 2008), it is imperative to examine its signature in the size distribution. For this the daily AOD values at each wavelength were arranged by grouping them in seasonal ensembles mean AOD spectra, representative of the different seasons were obtained. The

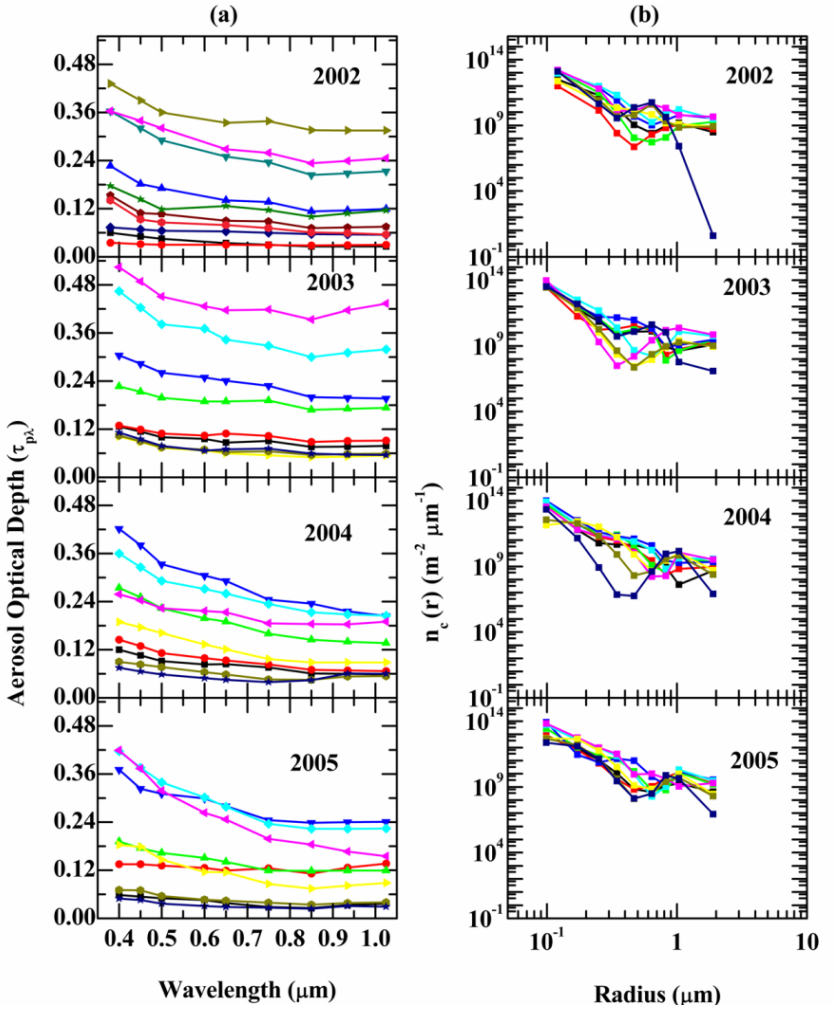

Fig. 3. Right panel (b) shows the composite plots of CSDs retrieved from the spectral AODs during 2002, 2003, 2004 and 2005. Left panel (a) shows the spectral AODs re-estimated from the retrieved CDSs (continuous line) along with the corresponding measured AOD spectra (points) that formed the inputs to the inversion.

seasonal size distributions were retrieved from these AOD spectra. The composite plots of CSDs during the winter and summer seasons are shown as composite plots respectively in Fig. 4 (bottom panels). In the top panels, the representative AOD spectra from the measurements are shown (solid points with error bars) along with the re-estimated $\tau_{p\lambda}$ (continuous line) values, using the retrieved size distributions as shown in the bottom panels. The nature of size distribution is almost similar during winter and summer seasons.

Physical Parameters of Aerosol from CSDs

With a view to quantifying the monthly and seasonal changes in the CSDs in terms of the physical parameters of aerosols, these CSDs are parameterized using appropriate analytical functions as discussed above, and the parameters like r_m, ν etc have been determined. The seasonal variations of the r_m and σ_m of the mode are shown in the lower and upper panels of Fig. 5, respectively. No systematic seasonal pattern is seen either in r_m or in σ_m. However, Fig. 5 indicates that the secondary coarse mode is broader and is generally consistent whereas the primary small/fine mode is explicitly not visible. In summer, the variability is either larger or comparable to those seen in other seasons.

With a view to examining the changes in columnar properties associated with the temporal changes in spectral AOD, the variation of the effective radius (R_{eff}), median radius (R), columnar mass loading (m_L), and columnar number concentrations of coarse mode aerosols N_c and total aerosols N_t are examined. Further, we have divided the N_t into two groups, the accumulation mode (small aerosol particles) and the coarse particles mode (larger aerosol particles) by integrating the CSDs, function from r_1 to 0.5 μm and from 0.5 μm to r_2 respectively. As the accumulation mode concentrations mainly pertains to the anthropogenic and transported (long range) species, while the coarse mode would represent mechanically generated particles, mostly due to the natural processes. As such the ratio N_c/N_a would represent a measure of the relative abundance of the number concentration of natural (coarse) aerosols N_c with respect to the anthropogenic abundance.

The temporal variations of monthly mean N_t, N_a, N_c and the ratio N_c/N_a are shown in Fig. 6 from bottom to top panels respectively. The accumulation mode particles N_a being larger than the coarse mode particles N_c by an order of magnitude, the ratio N_a/N_c is mainly determined by N_a. It was observed that during a year N_t, N_a, N_c and N_c/N_a increases from a minimum value during winter to a maximum value during summer months. An increase in the ratio of N_c/N_a clearly indicates the dominance of the coarse mode aerosols in the size spectrum during the summer seasons as compared to the winter season and it is considered to be responsible for flattening of the AOD spectrum

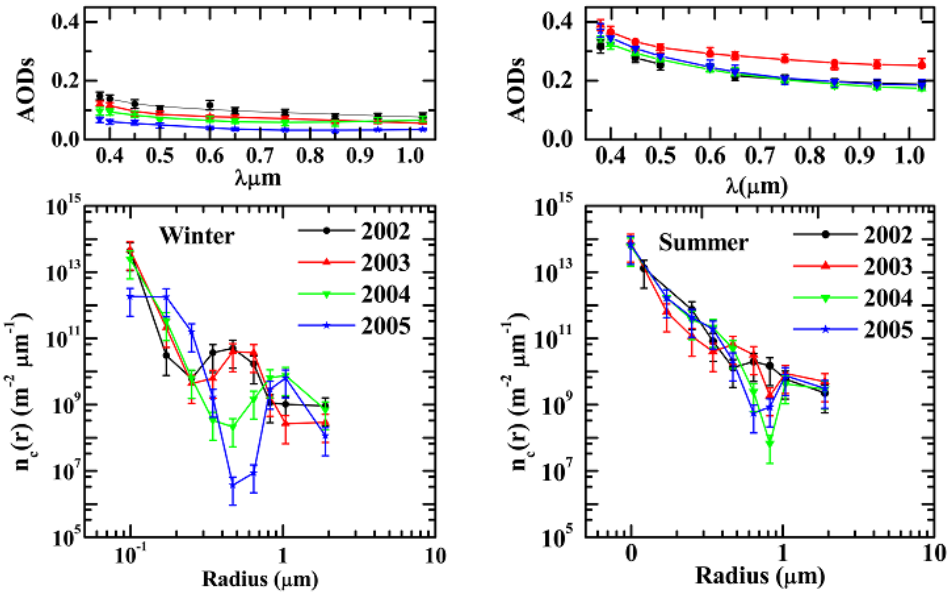

Fig. 4. Left top panel shows the input seasonal mean of $\tau_{p\lambda}$ values as estimated during winter seasons of every year (solid points with error bars), while the continuous lines shows the re-estimated $\tau_{p\lambda}$ values from the respective CSDs. The bottom left panel shows the seasonal CSD retrieved from the respective seasonal mean spectral AOD. Similar plots of seasonal mean $\tau_{p\lambda}$, re-estimated $\tau_{p\lambda}$ and CSD have been shown in the right top and bottom panels for summer season of every year.

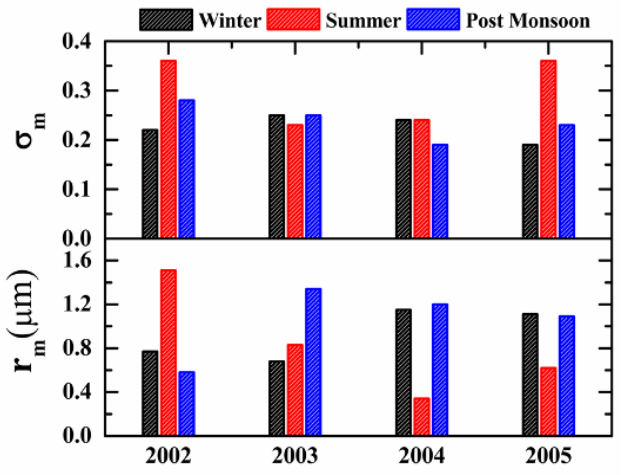

Fig. 5. The seasonal variation of mode radii and standard deviation of the mode radius.

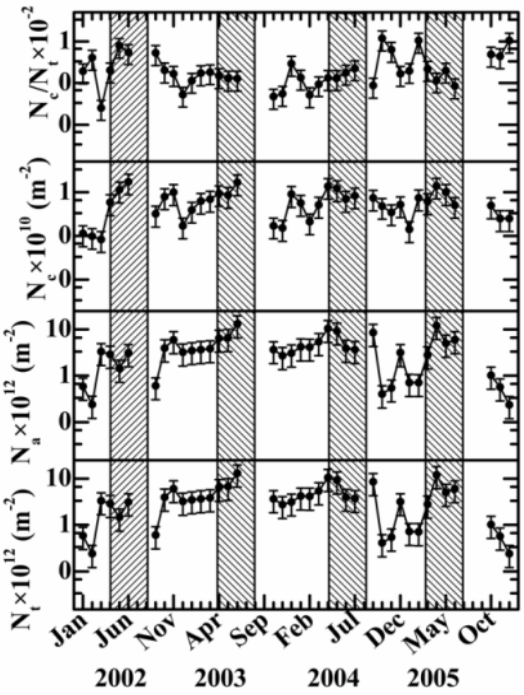

Fig. 6. Monthly variations of columnar aerosols content of the total (N_t) sub micron (N_a), super micron (N_c) and ratio (N_c/N_a) over Nainital during 2002 to 2005 are shown in the bottom to top panels respectively.

(Dumka *et al.,* 2008). Moreover, the total columnar abundance N_t also increases approximately by a factor of 10, as the season changes from winter to summer, indicating a large increase in the columnar abundance. This increase is more for N_c than for N_a and as a result the ratio N_c/N_a also increases. These results in a change in the aerosol spectrum which is also reflected in the effective radius (R_{eff}) and the columnar mass loading (m_L) as shown in the Fig. 7, which depicts the seasonal variation of R_{eff} and m_L in bottom and top panels respectively. Both m_L and R_{eff}, remain low during winter and high during summer. Though the seasonal variation of R_{eff} is not conspicuous during 2003 and 2004 but m_L shows the pattern consistently in all the years. The increase in the m_L and R_{eff} is attributed to the increase in the relative abundance of coarse aerosols in the size spectrum during the summer seasons. The value of R_{eff} depends on the relative dominance of large to small particles where as the value of m_L depends both on N_t as well as the concentration of coarse mode aerosols (Moorthy and Satheesh, 2000). As such, the relative abundance of large aerosol increases the value of R_{eff} while an increase in the columnar abundance of accumulation and coarse mode leads to an increase in m_L. As the R_{eff} is defined as the ratio of the total volume to area, the increase in the R_{eff} during the summer seasons is attributed to the increase in the relative abundance of coarse mode aerosol concentration. This partly

explains the absence of the constancy in R_{eff} from year to year. Further, during the summer there is a data scarcity due to the onset of monsoon over the experimental site which resulted to unequal weightage to the aerosol parameters in different years. The inter parameter dependencies are examined in Fig. 8, which shows a scatter plot of m_L and N_c/N_a against the R_{eff} in the bottom and top panels respectively. It is clearly seen that, the relative dominance of N_c (or N_c/N_a) leads to significant increase with the R_{eff} (Fig. 8; top panel) with a correlation coefficient of +0.53 at a significant level of 0.02. Similarly the columnar mass loading m_L is also positively correlated with R_{eff}; with a much lower correlation coefficient +0.38. These similarities with earlier observations indicate that R_{eff} is a batter proxy for monitoring the changes in the coarse mode abundance.

FN/AN Columnar Size Distributions

The aerosol measurements at Manora Peak, Nainital have shown that the AODs are found to be much lower as compared to the low altitude location in India (Sagar *et al.,* 2004; Dumka *et al.,* 2008). Further, afternoon (AN) AODs are generally higher than those of forenoon (FN) AODs, which was attributed due to the evolution of boundary layer, which transports aerosols and pollutants from the nearby polluted and valley (below the mountain peak) regions to the higher altitude. Further, the role of boundary layer dynamics in influencing the aerosol properties at Manora Peak using multi-year measurements of spectral aerosol optical depths during January 2002 to December 2004 are examined by Dumka *et al.* (2008). With a view to examining the implication of short period (within a daytime) fluctuations on the CSD and its parameters, we have retrieved CSDs separately for FN and AN hour's. The typical CSDs for FN and AN part of the day are shown in Fig. 9(b), for the month of November. Fig. 9(a) shows the monthly mean AOD values measured during FN and AN period at different wavelengths (solid points with error bars) along with the re-estimated AOD values from the corresponding size distributions (continuous line). In Fig. 9(b) $n_c(r)$ is plotted against r on a log-log scale and which is clearly shows that during AN hour's (when the boundary layer has fully evolved) the aerosol number density is higher than the FN hour's (when the boundary layer is shallow), though the nature of size distributions remains bimodal log normal distributions during both FN and AN periods, there is a slight shift in the position of occurrence of modes (secondary mode/coarse aerosols). The retrieved size distributions have been parameterized using bimodal log normal function, following the procedure outlines as above. The value of mode radius and standard deviation during the FN and AN periods are 0.78 ± 0.22 and 0.59 ± 0.35 respectively. This shows that the size distribution shifts towards the abundance of smaller/fine particles in AN hour's; probably due to influx of large quantities of fine aerosols induced into the column. The physical parameters for FN and AN periods are estimated from the corresponding size distributions and given in Table 1. The table shows that there is a significant increase in columnar concentration of total and accumulation mode aerosols in AN period (except in October) and consequently the R_{eff} of the size

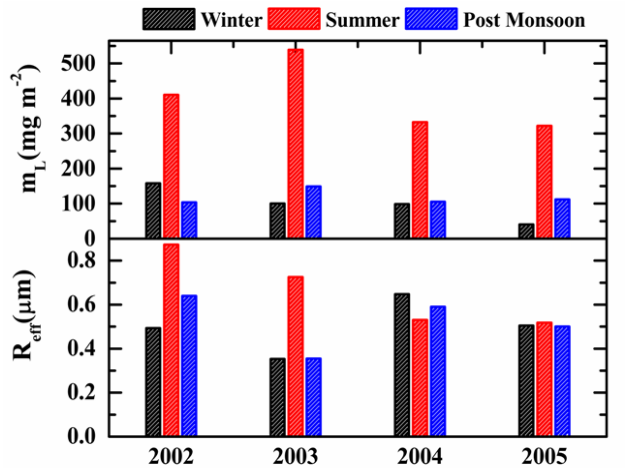

Fig. 7. The seasonal variation of m_L (top panel) and R_{eff} (bottom panel).

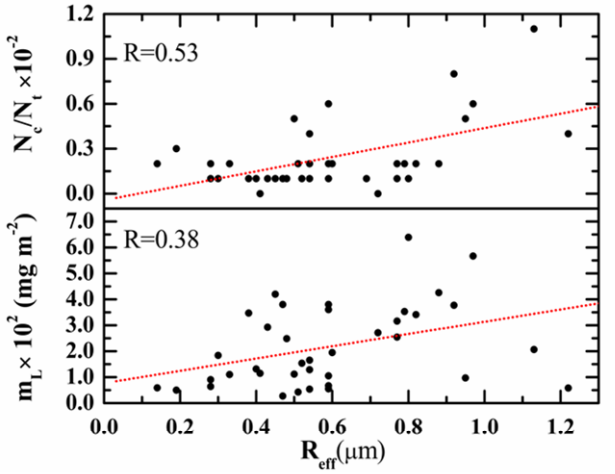

Fig. 8. Scatter plot of m_L and N_c/N_a against R_{eff} are shown in bottom and top panel respectively. The dotted line represents the linear fit of the points.

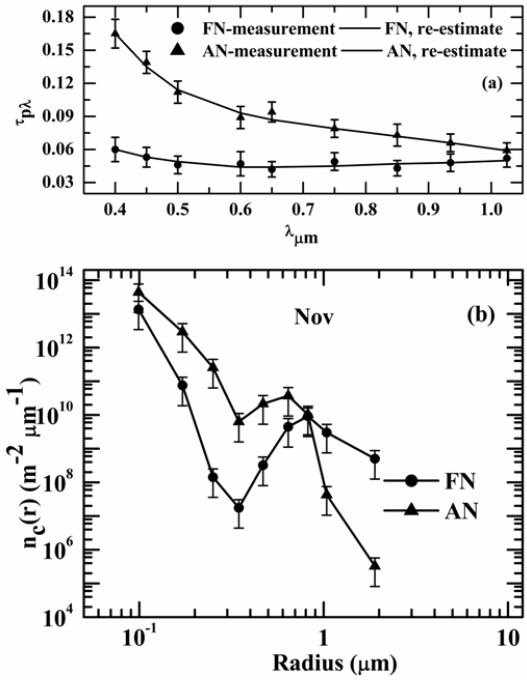

Fig. 9. (a) The input $\tau_{p\lambda}$ values estimated for FN and AN hour from the MWR measurements as the point with error. The continuous line represents $\tau_{p\lambda}$ values re-estimated using the retrieved CSDs. (b) typical example of FN and AN CSDs retrieved from monthly mean spectral AOD for the month of November at Nainital.

Table 1. The physical parameter of the FN and AN columnar size distributions during the study period.

Months	m_L *(mg/m²)*		R_{eff} *(μm)*		N_t (1/m³)		N_a (1/m³)		N_c (1/m³)		N_c/N_a	
	FN	AN	FN	AN	FN	AN	FN	AN	FN	AN	FN	AN
Jan.	54.16	100.73	0.20	0.25	4.41E+12	5.14E+12	4.41E+12	5.13E+12	3.29E+09	4.42E+09	7.49E-04	7.96E-04
Feb.	102.19	167.46	0.29	0.30	5.00E+12	6.26E+12	4.50E+12	6.25E+12	4.90E+09	9.44E+09	9.80E-04	1.50E-03
Mar.	233.47	245.44	0.83	0.24	2.35E+12	1.44E+13	2.35E+12	1.44E+13	1.92E+09	1.53E+10	8.17E-04	1.06E-03
Apr.	384.21	382.10	0.73	0.53	4.85E+12	6.88E+12	4.85E+12	6.87E+12	6.84E+09	1.21E+10	1.41E-03	1.76E-03
May.	554.27	435.01	0.94	0.35	4.33E+12	1.58E+13	4.14E+12	1.58E+13	6.10E+09	2.68E+10	1.41E-03	1.70E-03
Jun.	640.37	796.29	1.35	0.63	1.45E+12	1.66E+13	1.43E+12	1.66E+13	1.10E+10	8.09E+09	7.72E-03	4.87E-04
Jul.	--	--	--	--	--	--	--	--	--	--	--	--
Aug.	--	--	--	--	--	--	--	--	--	--	--	--
Sep.	--	--	--	--	--	--	--	--	--	--	--	--
Oct.	90.79	191.79	0.33	0.57	4.14E+12	3.18E+12	4.41E+12	3.18E+12	4.08E+09	2.02E+09	9.85E-04	6.36E-04
Nov.	69.16	61.38	0.48	0.17	1.75E+12	4.03E+12	1.75E+12	4.02E+12	4.04E+09	9.24E+09	2.31E-03	2.30E-03
Dec.	52.46	204.92	0.35	0.66	1.46E+12	2.63E+12	1.45E+12	2.63E+12	6.96E+09	3.40E+09	4.80E-03	1.29E-03

distributions. The effect is more spectacular during March to June period, when the solar heating of the land (over the Indo-Gangetic Plain) is quite intense leading to deeper convective mixing. This would lead to the lifting of effluents in the densely populated plains adjoining in the site to the higher levels, even above the peak, thereby inducting substantial amounts of urban aerosols in the column. Additional processes such as long range transport of fine mineral dust by the synoptic winds would also be playing their role during February to June months (e.g. Dey *et al.,* 2004; Hegde *et al.,* 2007; Nair *et al.,* 2007). Notwithstanding these the local boundary layer dynamics causes perceptible changes in aerosol characteristics (Dumka *et al.,* 2008). This is very important both in air quality assessment and aerosol characteristic to industrial urban areas where high altitude station lies close.

DISCUSSIONS

The CSDs retrieved from the measured AOD spectra consistently shows the bimodal (PL + UM) nature throughout the period under study from 2002 to 2004 (see Fig. 3). The similar type of size distribution is also reported by Rana *et al.* (2009). The wavelength dependency of AOD depicts a positive curvature towards the longer wavelength in the case of the bimodal nature of the size distribution. The secondary or coarse mode is generally occurring at a value of r > 0.5 μm, whereas the primary or fine mode is not conspicuous or occurring below the value of r < 0.1 μm, lower than the lower limit considered in the inversion technique. The occurrence of such mode suggests the presence of large abundance of nucleation (r~0.001 to 0.1 μm) or accumulation (r~0.1 to 1.0 μm) mode aerosols over the site. The occurrence of such mode is to be expected as the location is a remote, high altitude station lying in the central part of lower Himalayas and away from the strong sources of aerosol production. As the size spectrum is indicative of the particular source and sink of aerosols to which each mode can be attributed, therefore the bimodal nature of CSDs suggests two different sources of aerosols. However, the peak height of the secondary mode is almost 2-to-3 orders of magnitude less than that of the primary mode, which is not conspicuous (Fig. 2 & Fig. 3). Jaenicke (1984) and Hoppel *et al.* (1990) have suggested that the two modes observed in the CSDs are attributed mainly to two different production mechanisms: gas-to-particle conversion (GPC) and bulk-to-particle conversion (BPC) respectively. The primary small mode is attributed to the aged aerosols from the secondary GPC processes or phase reaction products as well as associated with the human activity on the landmass (Ramanathan *et al.,* 2001). The GPC gives rise to particles size of the order of radius < 0.5 μm, while the BPC gives rise to the larger sized particles of the order of radius > 0.5 μm. After the production, the fine particles (r~0.1 μm) of the size distribution are controlled mainly by the coagulation and condensation processes whereas the coarse mode particles (r > 0.5 μm) are mainly controlled by sedimentation (Pruppacher and Klett, 1978) and impaction scavenging processes. The nature of the size distribution between these radii limits reflects the aerosol sources, sinks and the aerosol transport, which have regional importance. As near the aerosol source, the aerosol characteristics are well associated to the generation or production mechanism while, it is quite different on a global or synoptic scale, when present at large distances from the source region. Moreover, the various microphysical processes bring out the continuous size transformations which are quite important in limiting the concentration of fine mode aerosols. The appearance of bimodal nature of CSDs is indicative of additional sources which are responsible for secondary mode aerosols. As the observational site Nainital is away from the major industrial or anthropogenic activities, the observed changes in the CSDs function are brought in terms of either natural sources and sinks or other long range transport mechanisms. The long range transport is capable of bringing large amount of desert and mineral aerosols from the west Asian and the Great Indian Desert to the site and is responsible for the generation of secondary mode during the study period over the site. In addition to the advection by air masses, the increased solar heating of the landmass in nearby plains and the under lying valley region adjacent to the measurement site during the summer season would result in the increased convection activity and the evolution of the atmospheric boundary layer (ABL) during daytime will cause lifting of the aerosols and pollutants to the higher altitudes. Hence the columnar content as well as the mass loading is increased during the summer seasons. Similar nature of size distribution is also reported near Indo-Gangetic basin by many investigators (Dey *et al.,* 2004; Singh *et al.,* 2004; Jethva *et al.,* 2005). They reported that the bimodal nature of the size distribution is due to the mixing of different type of air masses, having different aerosol populations (Hoppel *et al.,* 1985) and the long range transport from the Great Indian Desert.

CONCLUSIONS

The main conclusions of our study are the following:

1. Aerosol columnar aerosol size distributions retrieved from the inversion of spectral AOD, in general, show bimodal

(combination of power law and unimodal log normal) distributions, with a prominent secondary (coarse) mode occurring at fairly large value of r (> 0.5 μm), while the primary peak of fine mode aerosols does not appear explicitly. The basic shape of the CSD does not change significantly with the seasons.
2. There is an increase in the effective radius and columnar aerosol mass loading from winter to summer seasons, attributed to the increase in the relative dominance of coarse mode aerosols in the size spectrum during the summer season.
3. The aerosol physical parameters estimated from the CSDs have minimum values during the winter seasons and maximum during summer months.
4. The share of sub micron aerosol to the aerosol number concentration shows the dominant role of sub micron aerosols to the total aerosol number concentration and it accounts for > 90% during the study period, which indicates that the sub micron aerosols contribute significantly to the aerosol loading during the study period.

ACKNOWLEDGEMENTS

This work was carried out as a part of Indian Space Research Organization, Geosphere Biosphere Program. The authors would like to express their sincere gratitude to Dr. Brijesh Kumar for fruitful discussion and all the technical staff of ARIES, for providing the valuable help during the observations. Authors are also grateful to anonymous reviewers for their constructive and useful suggestions.

REFERENCES

Ackerman, A.S., Toon O.B., Stevens D.E., Heymsfield A.J., Ramanathan V. and Welton E.J. (2000). Reduction of Tropical Cloudiness by Soot. *Science*. 288: 1042-1047.

Charlson, R.J., Schwartz, S.E., Hales, J.M., Cess, R.D., Coakley, J.A., Hansen, J.E. and Hoffmann, D.J. (1992). Climate Forcing by Anthropogenic Aerosols. *Science*. 255: 423-430.

Charlson, R.J., Lovelock, J.E., Andreae, M.O. and Warren, S.G. (1987). Oceanic Phytoplankton, Atmospheric Sulfer, Cloud Albedo and Climate. *Nature.* 326: 655-661.

Dey, S., Tripathi, S.N., and Singh, R.P. (2004). Influence of Dust Storms on the Aerosol Optical Properties over the Indo-Gangetic Basin. *J. Geophys. Res.* 109: D20211.

Dumka, U.C., Moorthy, K. Krishna, Satheesh, S.K., Sagar, R. and Pant, P. (2008). Short-Period Modulations in Aerosol Optical Depths over Central Himalayas: Role of Mesoscale Processes. *J. Climate Appl. Meteor.* 47: 1467-1475.

Ganesh, K.E., Umesh, T.K., and Narasimhamurthy, B. (2008). Site Specific Aerosol Optical Thickness Characteristics over Mysore. *Aerosol Air Qual. Res.* 8: 295-307.

Gogoi M.M., Moorthy, K.K., Babu, S.S., and Bhunyan, P.K. (2009). Climatology of Columnar Aerosol Properties and the Influence of Synoptic Conditions-First Time Results from the Northeastern Region of India. *J. Geophys. Res.* 114: D08202.

Hegde, P., Pant, P., Naja, M., Dumka, U.C. and Sagar, R. (2007). South Asian Dust Episode in June 2006: Aerosol Observations in the Central Himalayas. *Geophys. Res. Lett.* 34: L23802.

Hoppel, W.A., Fitzgerald, J.W., and Larson, R. E. (1985). Aerosol Size Distributions in Air Masses Advecting off the East Coast of the United States. *J. Geophys. Res.* 90: 2365-2379.

Hoppel, W.A. Fitzgerald, J.W., Frick, G.M. and Larson, R.F. (1990). Aerosol Size Distribution and Optical Properties Found in the Marine Boundary Layer over the Atlantic Ocean. *J. Geophys. Res.* 95: 3659-3686.

Jaenicke, R. (1984). *Physical Aspects of Atmospheric Aerosol, Aerosols and Their Climate Effects*, H.E. Gerbard and A. Deepak (Eds). A Deepak Publishing. p. 7-34.

Jethva, H., Satheesh, S.K., and Srinivasan, J. (2005). Seasonal Variability of Aerosols over the Indo-Gangetic Basin, *J. Geophys. Res.* 110: D21204.

Junge, C.E. (1963). *Air Chemistry and Radioactivity*, Academic Press, New York.

King M.D. (1982). Sensitivity of Constrained Linear Inversion to the Selection of Lagrange Multiplier. *J. Atmos. Sci. 39:* 1356-1369.

King M.D., Byrne, D.L., Herman B.M., and Reagan, J.A. (1978). Aerosol Size Distributions Obtained by Inversion of Spectral Optical Depth Measurements. *J. Atmos. Sci.* 35: 2153-2167.

Künzli N., Kaiser, R., Medina, S., Studnicka, M. *et al.* (2000). Public-health Impact of Outdoor and Traffic-related Air Pollution: a European Assessment. *Lancet*. 356: 795-801.

Moorthy, K.K. and Satheesh, S.K. (2000). Characteristics of Aerosols over a Remote Island, Minicoy in the Arabian Sea: Optical Properties and Retrieved Size Characteristics. *Quart. J. Roy. Meteor. Soc.* 126: 81-109.

Moorthy, K.K., Nair P.R. and Murthy, B.V.K. (1991). Size Distribution of Coastal Aerosols: Effects of Local Sources and Sinks. *J. Appl. Meteor.* 30: 844-852.

Moorthy, K.K., Satheesh, S.K. and Murthy, B.V.K. (1997). Investigations of Marine Aerosols over the Tropical Indian Ocean. *J. Geophys. Res.* 102: 18827-18842.

Nair, P.R., and Moorthy, K.K. (1998). Effects of Changes in the Atmospheric Water Vapour Content on the Physical Properties of Atmospheric Aerosols at a Coastal Station. *J. Atmos. Terr. Phys.* 60: 563-572.

Nair, V.S., Moorthy, K.K., Alappattu, D.P. *et al.* (2007). Wintertime Aerosol Characteristics over the Indo-Gangetic Plain (IGP): Impacts of Local Boundary Layer Processes and Long-range Transport. *J. Geophys. Res.* 112: D13205.

Pant, P., Hegde, P., Dumka, U.C., Sagar, R., Satheesh, S.K., Moorthy, K.K., Saha, A., and Srivastava, M.K. (2006). Aerosol Characteristics at a High Altitude Location in Central Himalayas: Optical Properties and Radiative Forcing. *J. Geophys. Res.* 111: D17206.

Pruppacher, H.R. and Klett, J.D. (1978). *Microphysics of Clouds and Precipitation*, D. Reidel Publishing Company, Holland.

Ramanathan, V., Crutzen, P.J., Lelieveld, J. *et al.* (2001). Indian Ocean Experiment: An Integrated Analysis of the Climate Forcing and Effects of the Great Indo-Asian haze. *J. Geophys. Res.* 106: 28371-28398.

Rana, S., Kant, Y. and Dadhwal, V.K. (2009). Diurnal and Seasonal Variation of Spectral Properties of Aerosols over Dehradun, India. *Aerosol Air Qual. Res.* 9: 32-49.

Rosenfeld, D. (2000). Suppression of Rain and Snow by Urban and Industrial Air Pollution. *Science.* 287: 1793-1796.

Russell, L.M., Pandis, S.N. and Seinfeld, J.H. (1994). Aerosol Production and Growth in Marine Boundary Layer. *J. Geophys. Res.* 99: 20989-21003.

Sagar, R., Kumar, B., Dumka, U.C., Moorthy, K.K., and Pant, P. (2004). Characteristics of Aerosol Spectral Optical Depths over Manora Peak: A High-altitude Station in the Central Himalayas. *J. Geophys. Res.* 109: D06207.

Satheesh, S.K., Ramanathan, V., Jones, X.L., Lobert, J.M., Podogorny, I.A., Prospero, J.M., Holben, B.N. and Leob, N.G. (1999). A Model for Natural and Anthropogenic Aerosols for Tropical Indian Ocean Derived from Indian Ocean Experiment Data. *J. Geophys. Res.* 104: 27421-27440.

Saha, A. and Moorthy, K.K. (2004). Impact of Precipitation on Aerosol Spectral Optical Depth and Retrieved Size Distributions: A Case Study. *J. Appl. Meteor.* 42: 902-914.

Shettle, E.P. and Fenn, R.W. (1979). Models for the Aerosols of Lower Atmosphere and the Effect of Humidity Variations on Their Optical Properties. AFGL-TR-79-0214, Environmental Research Paper No. 675, 26pp, Phillips Lab, Hanscom Air

Force Base, Mass.

Singh, R.P., Dey, S., Tripathi, S.N. and Tare, V. (2004). Variability of Aerosol Parameters over Kanpur, Northern India. *J. Geophys. Res.* 109: D23206.

Srivastava, A.K., Devara, P. C. S., Rao,Y. Jaya, Bhavanikumar, Y. and Rao, D.N. (2008). Aerosol Optical Depth, Ozone and Water Vapour Measurements over Gadanki, a Tropical Station in Peninsular India. *Aerosol Air Qual. Res.* 8: 459-476.

Twomey, S.A. (1977). The Influence of Pollution on the Short-Wave Albedo of Clouds. *J. Atmos. Sci.* 34: 1149-1152

Received for review, January 11, 2009
Accepted, March 2, 2009